Yellowing of laser-cleaned artworks: Formation of residual hydrocarbon compounds after Nd:YAG laser cleaning of gypsum plates covered by lamp black

Jérémie Berthonneau, Philippe Parent, O. Grauby, Daniel Ferry, Carine Laffon, Alain Colombini, Blandine Courtois, Philippe Bromblet

Yellowing of laser-cleaned artworks: formation of residual hydrocarbon compounds after Nd:YAG laser cleaning of gypsum plates covered by lamp black.

Jeremie BERTHONNEAU[1*], Philippe PARENT[1*], Olivier GRAUBY[1], Daniel FERRY[1], Carine LAFFON[1], Alain COLOMBINI[2], Blandine COURTOIS[1] and Philippe BROMBLET[2]

[1] Aix-Marseille Université, CNRS – UMR 7325 CINaM (Centre Interdisciplinaire de Nanoscience de Marseille), Campus de Luminy, 13288 Marseille Cedex 9, France.

[2] CICRP Belle de Mai, 21 rue Guibal, 13003 Marseille, France.

Title:

Yellowing of laser-cleaned artworks: formation of residual hydrocarbon compounds after Nd:YAG laser cleaning of gypsum plates covered by lamp black

Detailed plan of the article:

Abstract:

The removal of black crusts decaying the surface of artworks is an important concern for the conservation of cultural heritage. Nd:YAG laser cleaning of encrusted stones and plasters at 1064 nm is widely recognized as an effective restoration technique, but induces a noticeable yellowing of the surface. Several researches carried out on the effects of laser cleaning have been focused on the induced yellowing and how to visually mitigate this phenomenon. To this end, UV-B radiations were successfully used to lessen the laser-induced yellowing due to the removal of lamp black particles on gypsum. The mechanism at play for both the formation of the compounds yellowing the surface and their disappearance upon UV-B exposure remains, however, poorly understood. Within the frame of this research, we apply surface-sensitive characterization techniques to analyze the yellowed surface produced after Nd:YAG Q-Switched laser cleaning of lamp black deposit on a gypsum plate, and the same surface after UV-B exposure. A combination of X-ray photoelectron spectroscopy and Fourier-transformed infrared spectroscopy has been used to identify the residual carbon compounds responsible for the yellow coloration of the substrate. A nanoscale structural description of the ejected particles collected during the laser cleaning was finally performed with transmission electron microscopy. We found that the yellowing is due to partially oxidized hydrocarbons compounds deposited at the surface of the gypsum substrate. We propose that they form by reactions between carbon species emitted by the vaporization of the carbon particles, with hydrogen and oxygen produced by the dissociation of water molecules coming together from dehydration of the gypsum surface and from the water sprayed by the operator during cleaning.

Keywords:

Black crust/Laser cleaning/ XPS/FTIR/Electron microscopy/Restoration

1. Introduction

Laser cleaning in restoration of artworks is a well-established and optimized technique [1,2]. Criticisms have, however, been expressed after its implementation due to the yellowish tint of the laser cleaned surfaces [3]. The phenomenon thus became a controversial issue as it was unclear whether it resulted from a specific side effect of laser cleaning [4] or from the revealing of a preexisting yellowish layer [5,6]. Many scientific investigations recently evidenced laser irradiation as the cause of the yellowing process and proposed ways to mitigate the discoloration pattern using poultices [7] or UV-B irradiation [8]. Nevertheless, the chemical composition as well as the formation mechanism of the compounds yellowing the surface remain enigmatic. As recently pointed out: "*the exact nature of the material generated by laser treatment of black crust and contributing to the yellow color is still unknown*" [9]. Several obstacles preclude the investigations. The material, phase or impurities at the origin of the yellowing are invisible and hardly analyzable using conventional techniques on thin sections. When analyses are carried out at the surface, only the substrate compounds are revealed without recognition of any neoformed phases [1,2,9]. The phases induced by laser cleaning are therefore assumed to be nano-sized and in a very low amount.

Black crusts forming at the interface between the substrate, the atmosphere and the polluted urban or industrial environment, have very complex compositions ranging from nano to sand size particles, minerals and organics, with a long list of chemical elements that are combined in various ways [5,10]. The interactions that may occur during a laser pulse are complex and the distinction between the initial black crust compounds and neoformed phases resulting from laser irradiation is far from obvious. A way to experimentally reproduce the phenomenon at play is (i) to make synthetic gypsum substrate, close to the epigenic gypsum layer systematically found beneath the black crust on carbonate stone surface [8,9], (ii) to artificially cover this substrate with a layer containing a single specie sensitive to the laser, and (iii) to study the residues present on the yellowed surface after laser irradiation. Such model systems have been investigated by various authors, using a multi-scale approach from optical to electron microscopy coupled with energy-dispersed X-ray as well as electron energy loss spectroscopy to study the morphological, mineralogical and chemical features that could be linked to the yellowing

phenomenon [8,9,11,12]. These studies brought new insights on the involvement of iron compounds and fly ashes in the yellowing phenomenon. Researches also showed that black crusts can be mimicked by lamp black nanoparticles, and that the laser-induced yellowing phenomenon is mitigated by UV-B irradiation [8,11]. The different processes at play along these treatments of gypsum plates covered with lamp black particles were carefully followed by spectrocolorimetry, but no information concerning the composition of the laser-induced yellow surface were gained up until now. Following this work, we have developed a specific analytical protocol capable of characterizing primary as well as neoformed nano-sized phases of lamp black upon the different treatments. A combination of X-ray photoelectron spectroscopy (XPS), Fourier-transform infrared spectroscopy (FTIR), scanning electron microscopy (SEM), and transmission electron microscopy (TEM) was applied to follow the chemical and morphological changes of a gypsum plate covered with lamp black, exposed to Nd:YAG Q-Switched laser cleaning at 1064 nm followed by UV-B irradiation at 313 nm. These investigations bring new insights on the nature and origin of the laser-induced yellowing phenomenon.

2. Research aims

Beside its unquestionable advantages, the Nd:YAG laser cleaning of artworks yields to the yellowing of the treated surfaces. This study thus aims at understanding the mechanism at play in the laser-induced yellowing phenomenon by providing morphological, chemical, and structural characterizations of the primitive and the neo-formed carbon species on a model system. The ultimate objective consists in providing physico-chemical justifications for the simultaneous or consecutive use of UV-B exposure allowing for the progressive removal of the carbon compounds involved in the yellowing phenomenon.

3. Materials and methods

3.1 Sample preparation: Synthetic samples were elaborated with gypsum plaster plates manually covered with a thin layer of lamp black particles. The gypsum plates were made by hydration of pure

hemihydrate (97%, Acros organics) with distilled water (1/1 in mass). Windows (76 x 26 mm) were cut in a dense foam template and glass microscope slides were placed at the bottom. The mixture (hemihydrate + distilled water) was then applied on the slides until the windows were filled. The surface was finally leveled with a spatula and the samples were left to dry for at least 24 hours. After demolding, the surface was covered with lamp black pigment (noir de fumée ©) supplied by Artech. Fine-grained black powder was applied dry with a brush to cover the gypsum plate with a black layer.

3.2 Laser cleaning: The plates were first cleaned with a Nd:YAG Q-Switched (QS) laser at 1064 nm (Thomson BM Industries NL201, 8 mm spot beam, 15 ns pulse duration, 10 Hz pulse frequency). The laser fluence, expressed as an energy per unit area of the beam, ranged from 200 to 400 mJ/cm$_2$. The irradiation conditions have been adjusted by an experienced restorer to optimize the cleaning result. The surface of the samples was sprayed with water just before irradiation. Around a quarter of each sample was preserved from laser cleaning and kept as a reference area (Area 1 in Fig. 1). A complementary laser cleaning was carried out in the same conditions in order to collect the ablated particles during laser irradiation. In this case, the sample was inclined at 45° in a box and small metal grids used for transmission electronic microscope observation were held close to it during the cleaning operation.

3.3 UV-B exposure: After laser cleaning, the plates were exposed to UV-B radiation (313 nm) in an accelerated UV degradation chamber (Q-Panel LAB product) following previously optimized conditions [8]: 90 hours at an irradiance of 1.42 W/m$_2$ reaching a total UV-B fluence of 46 J/cm$_2$. A second quarter of the sample was protected with an aluminum foil to preserve the yellowed surface obtained after laser cleaning (Area 2 in Fig. 1). The UV-B exposed surface represents the rest of the sample (Area 3 in Fig. 1).

3.4 Spectrocolorimetry: Color measurements were carried out with a Hunterlab MiniScan XE Plus System spectrocolorimeter with illuminant D65 using the 10° observer, equipped with a hand-held positioning device [8], to evaluate the color variations after QS laser cleaning (Area 2 in Fig. 1) and UV-B exposure versus time (Area 3 in Fig. 1). The evolution of the b* parameter, representative of the chromaticity of interest, was specifically followed with respect to the gypsum reference surface.

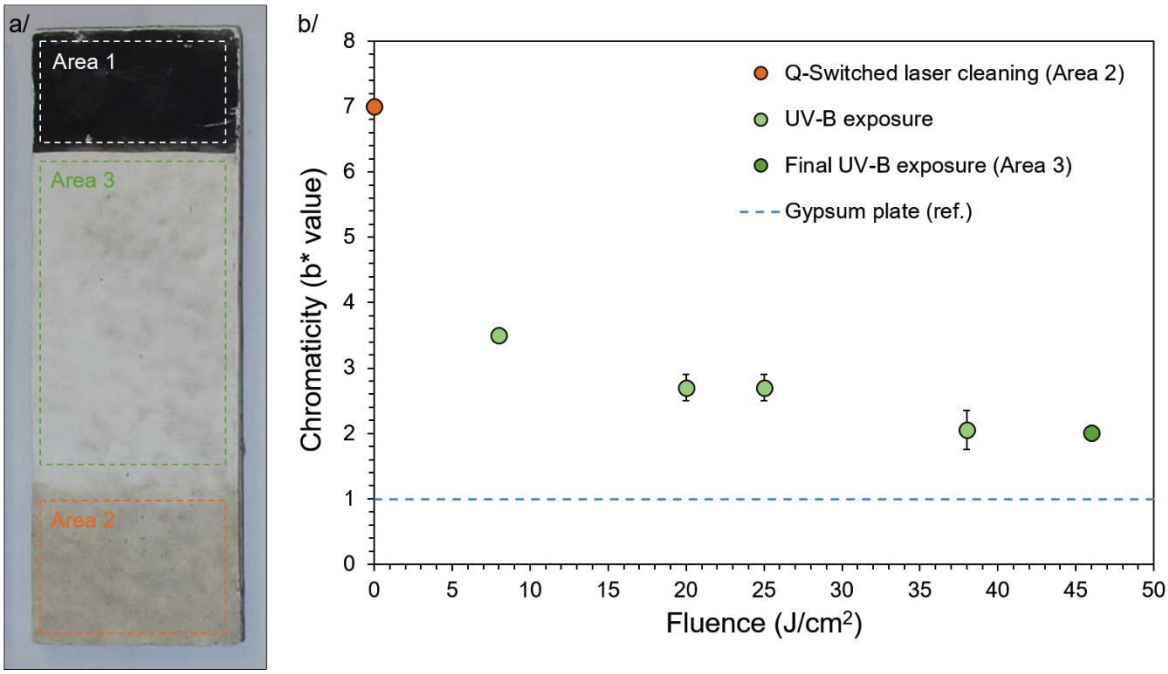

Figure 1. a/ Macroscopic color changes of a gypsum plate covered with lamp black (Area 1) after Q-Switched laser cleaning (Area 2) and UV-B exposure (Area 3). The plate is 7.5 cm long. b/ Chromatic evolution of the Q-Switched laser cleaned area (b* value) as function of the cumulated UV-B fluence. The dashed blue line corresponds to the b* value measured on the reverse side of the gypsum plate.

3.5 X-ray photoelectron spectroscopy: XPS was recorded on Areas 1-3 to characterize the elemental composition and the chemical speciation of the surface species. Reference spectra were also acquired on a bare gypsum plate and on the lamp black powder for comparison purposes. The experiments were performed under ultra-high vacuum using a Resolve 120 hemispherical electron analyzer (PSP Vacuum) and a TX400 (PSP vacuum) unmonochromatized X-ray source (Mg Kα at 1253.6 eV) operated at 100 W. The information depth of XPS at this excitation energy and in the geometrical arrangement of the setup is typically 1 nm at the C1s line. Survey spectra were first collected at pass energy of 50 eV and an energy step of 0.2 eV, while the C1s lines were collected at 20 eV pass energy, and a step of 0.1 eV. The XPS lines were deconvoluted with the CasaXPS program, using Gaussian/Lorentzian profiles and after Shirley-type background subtraction. Elemental composition (in at. %) are obtained from the analysis of the survey spectra and after correction by the relative sensitivity factors provided in the program.

3.6 Fourier-transform infrared spectroscopy: the infrared spectra were recorded in attenuated total reflectance (ATR, germanium crystal) mode using a Bruker VERTEX70 mid-IR Fourier Transform

spectrometer equipped with a temperature-stabilized DLaTGS detector. All spectra were accumulated on the surface of the different areas as well as the reference materials (bare gypsum plaster and lamp black) in a spectral range of 650-4000 cm^{-1} by recording 200 scans at a resolution of 4 cm^{-1}. In this energy domain, information depth in ATR is in the range of 0.2-1.4 μm for gypsum, i.e. 200-1400 times deeper than XPS. The Opus software was used for the baseline correction, where a polynomial fit was applied over the whole spectral range with a minimal number of anchor points (between 3 and 5, typically). The characterization of the absorbance bands and the interpretation of their evolution with the different treatments were carried out by a curve fitting procedure using the PeakFit software. We have selected two regions of interests (ROIs) where specific spectral features of carbon are observed, corresponding to the intervals between 1300 and 1600 cm^{-1} and between 2800 and 3100 cm^{-1}. The ROIs were adjusted with several absorbance bands with Voigt profiles. Such profile is common in complex condensed materials and corresponds to a convolution of Lorentzian and Gaussian profiles. The fitting was achieved using a least-squares iterative procedure by varying the peak position, amplitude/area, Gaussian and Lorentzian half-widths for all absorbance bands.

3.7 Scanning electron microscopy and transmission electron microscopy: SEM was used to study the morphology of the lamp black particles, the gypsum plaster substrate, and the treated areas at a micron and sub-micron scale. The SEM observations were performed with a JEOL 6320F operated at 15kV. Samples were coated with titanium prior to being placed in the SEM chamber. TEM was performed to characterize the nanoscale morphology and internal structure of the particles composing the lamp black and the ablated particles collected on the grids during cleaning tests. TEM observations were carried out on a JEOL JEM 2011 operated at 200kV. Bright field TEM micrographs were acquired with a CCD camera (GATAN, Ultrascan® 1000XP) assisted by the Digital Micrograph software (GATAN).

4. Results

Visual observation (Fig. 1a) allows an easy distinction of the three different areas (Area 1/lamp black crust, Area 2/after Q-Switched laser cleaning, and Area 3/after 90 hours of UV-B exposure). After

182 laser cleaning, Area 2 has a yellowish aspect, with a b* value of about 7 in term of chromaticity. It
183 corresponds to the b* value at zero UV-B fluence (Fig. 1b). The evolution of b* indicates the
184 colorimetric changes induced by UV-B exposure of Area 3. Colorimetric measurements were made
185 repetitively on this area after 15, 40, 50, 70, and 90 hours of exposure. The decrease of b* highlights the
186 progressive de-yellowing phenomenon previously described [8,11]. However, b* does not reach the
187 reference value of 0.99 (dashed line in Fig. 1b) within the considered exposure time, indicating that UV-
188 B exposure does not fully reveal the original color of the gypsum plate.

189 The deconvoluted C1s XPS spectra recorded on Areas 1-3 are shown in Fig. 2a (the C1s and O1s
190 spectra, including those of the bare gypsum plate and the lamp black particles are presented and further
191 discussed in the supplementary material S1). The black crust of Area 1 (Fig. 2a, bottom) presents a main
192 peak located at a binding energy of 284.8 eV corresponding to the lamp black particles, and typical of
193 graphitic materials [13]. The second peak at 288.2 eV is related to carbonate CO_3, likely in the form of
194 calcium carbonate $CaCO_3$ [14] contaminating the gypsum plate surface, a contamination of unknown
195 origin. It is already present on the bare gypsum spectrum (see supplementary material S1) and is detected
196 in Area 1 as the substrate is not perfectly covered by the carbon crust (see below, SEM results, Fig.5a).
197 The lamp black peak contributes to 49 at. % to the elemental surface composition of Area 1 (Fig. 2b).
198 After laser cleaning (Area 2) the carbonate peak at 288.2 eV has increased relatively to the other
199 contributions (Fig. 2a, middle). The residual carbon peak, now shifted at 285.5 eV, represents only 4 at.
200 % of the elemental composition of Area 2 (Fig. 2b). This + 0.7 eV shift indicates that this residual carbon
201 is not of the same kind than the initial lamp black particles. Binding energies of 285.5 eV correspond to
202 aliphatic hydrocarbons [15], which therefore dominate the composition of the residual carbon layer. A
203 further C1s peak at 291.6 eV appears, typical of CO_2 [16]. We assume that a part of the $CaCO_3$ species
204 located at the very surface (typically 1 nm in depth) have been decomposed in $CaO + CO_2$ [17] under
205 the laser beam. CO_2 remains trapped in the subsurface region, perhaps through chemical complexation
206 or in nano-bubbles. As this reaction takes place at T°> 800°C, it allows setting at 800 °C the lower
207 temperature experienced by the first atomic layers of the gypsum surface during the laser treatment.

208 After UV-B exposure (Area 3, Fig. 2a top), the residual carbon peak at 285.5 eV has almost totally
209 disappeared. The remaining signal represents only 0.75 ± 0.15 at. % (rounded at 1 at. % Fig.2b) of the
210 elemental composition of Area 3 (Fig. 2b), while the $CaCO_3$ and the CO_2 peaks are still present. UV-B
211 induces the removal of the residual carbon compounds, which eventually whitens the gypsum surface
212 [8,11]. We suppose that this 1 at. % of remaining carbon precludes the full recovery of the original
213 chromaticity of the gypsum plate (Fig. 1b).

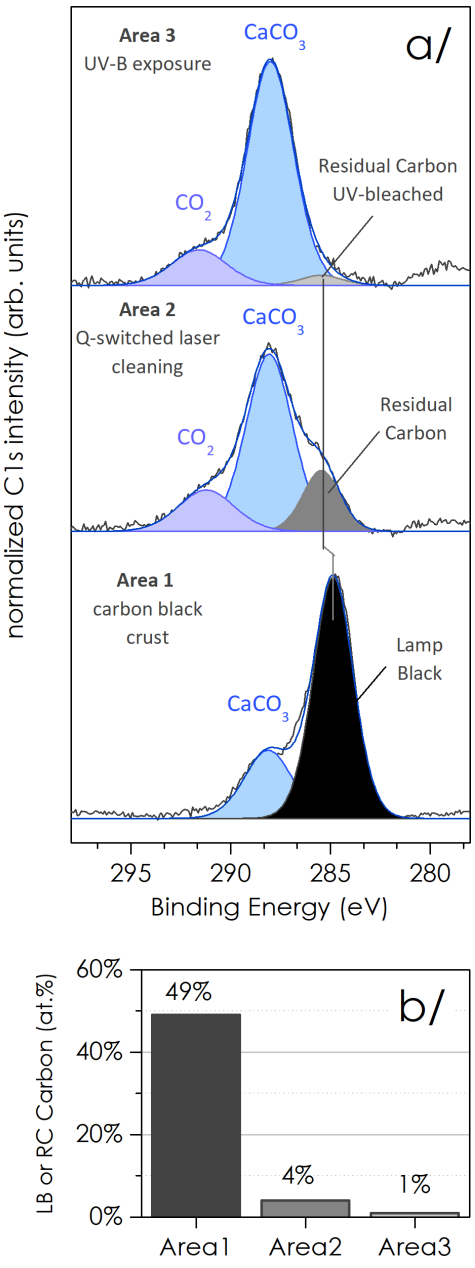

Figure 2. a/ Deconvoluted C1s XPS lines of Areas 1-3. b/ Contributions to the total surface composition (in at. %) of the lamp black (LB) C1s line in Area 1, and of the residual carbon (RC) C1s lines in Area 2 and 3.

214 The FTIR spectra of the gypsum substrate and those of Areas 1-3 are displayed in Fig. 3, after baseline
215 subtraction and normalization by their integrated area. The most intense absorption bands come from
216 the bending (δ) and stretching (υ) vibration of gypsum, located at 1010 (υ_1 SO_4), 1150 (υ_3 SO_4), 1620

(δ O-H··O), 1680 (δ O-H··O), 3240 (υ O-H··O), 3410 (υ O-H··O), and 3550 cm^{-1} (υ O-H··O) [18]. Very weak bands coming from CH and CC vibrations are also present but barely distinguishable on Fig. 3.

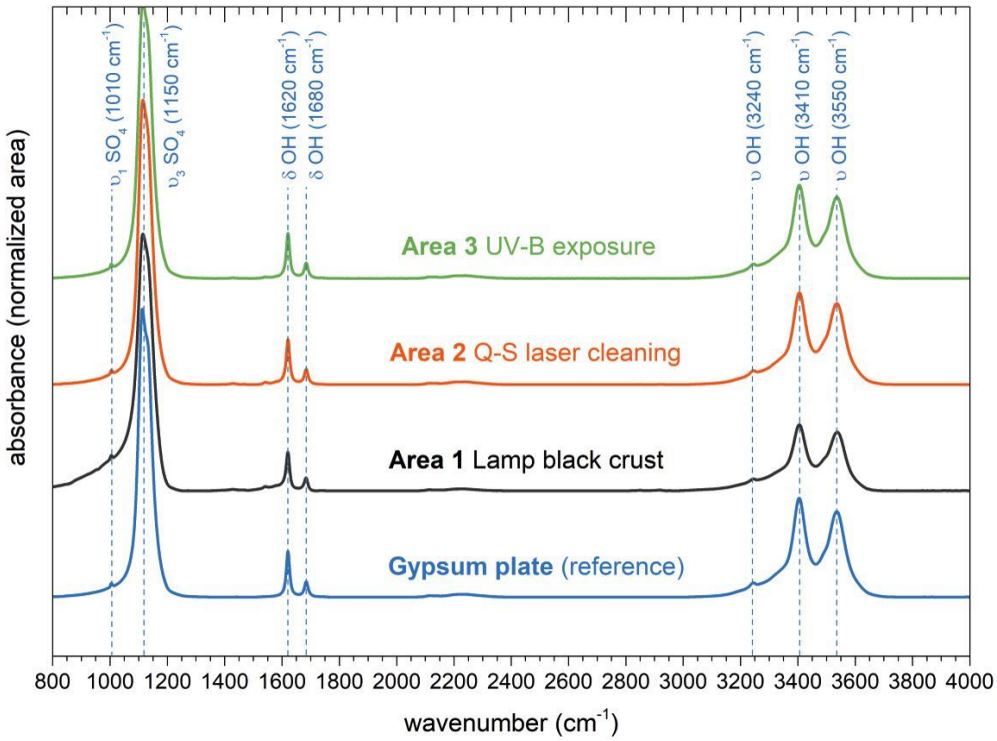

Figure 3. Baseline corrected ATR-FTIR spectra obtained on the reference gypsum plate and areas 1-3.

The CH and CC vibrations can be studied on the two ROIs (1300-1600 cm^{-1} and 2800-3100 cm^{-1}) presented Fig. 4a and 4b where the spectral intensities have been renormalized to the gypsum bands at 1680 cm^{-1} (Fig. 4a) and 3410 cm^{-1} (Fig. 4b). In the 1300-1600 cm^{-1} region (Fig. 4a), these bands are assigned to the C-H bending bands of aliphatic compounds (δ CH_3 sym. ~1390 cm^{-1}; δ CH_2 ~ 1430 cm^{-1}; δ CH_3 asym. ~ 1470 cm^{-1}) and to the stretching bands of aromatic rings (υ C=C ~ 1540 and 1600 cm^{-1}) [19]. In the 2800-3100 cm^{-1} region (Fig. 4b), the absorption bands are assigned to the C-H stretching bands of aliphatic and aromatic compounds (υ CH_2 bridges ~ 2825 cm^{-1}; υ CH_2 sym. ~ 2850 cm^{-1}; υ CH_3 sym. ~ 2875 cm^{-1} υ CH ~ 2895 cm^{-1}; υ CH_2 asym. ~ 2920 cm^{-1}; υ CH_3 asym. ~ 2960 cm^{-1}, υ CH aromatic at 3030 cm^{-1}) [19,20]. These organic compounds are present in the lamp black particles, made of a mixture of small bent graphitic crystallites (see below, TEM results) and matrix-bonded hydrocarbons. Assuming that the substrate bands remain unaltered by the different treatments on the depth probed by the ATR technique, the normalization allows estimating the relative changes in the carbon coverages

232 with the different treatments. A spectral deconvolution of the FTIR signal is therefore presented in Fig.
233 4 for the two ROIs.

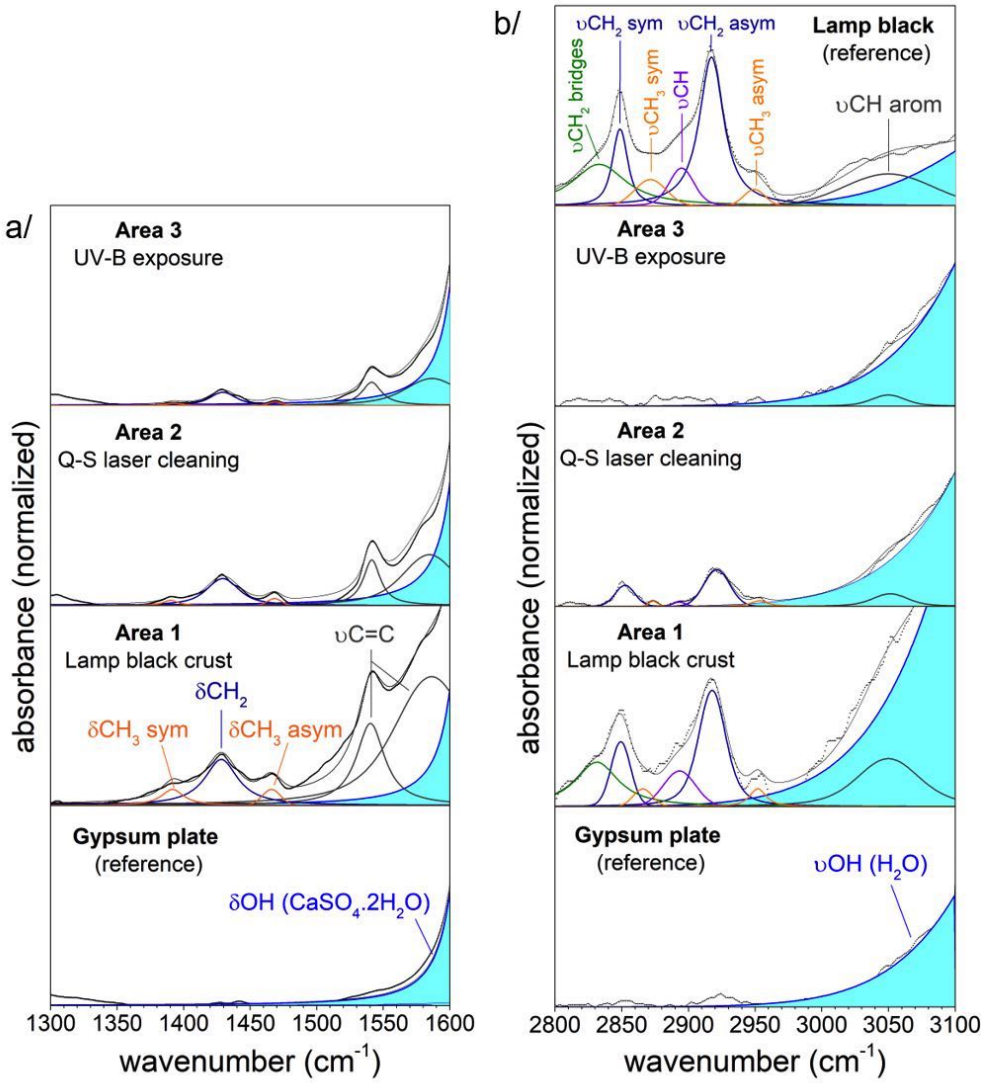

Figure 4. Contribution of the different vibrational modes on the curve fitting analysis of regions a/ 1300-1600 cm^{-1} and b/ 2800-3100 cm^{-1}. The reference spectrum of the lamp black powder was also fitted in the 2800-3100 cm^{-1} domain for comparison.

234 In Area 1 the prevalence of the two absorption bands at 2850 and 2925 cm^{-1} (CH_2 symmetric
235 and asymmetric stretching modes, in blue lines on Fig. 4b) with respect to those of the CH_3 groups
236 terminating the aliphatic chains (in orange lines) indicates that these chains are long. The band at 2895
237 cm^{-1} (in purple line on Fig. 4b) is related to C-H stretching of tertiary carbon atom at branching points
238 of the aliphatic chains [20]. The absorption band at 2825 cm^{-1} is assigned to CH_2 groups located near
239 sp_2-hybridized carbon (in green on Fig. 4b), for instance in aliphatic species bonded to (or binding) the
240 edge(s) of the graphitic crystallites [20]. This band is not detected anymore in the spectrum of Area 2,
241 indicating that these peripheral CH_2 groups have disappeared after the laser impact. This is a further

evidence, with XPS, that the structure of the residual carbon compounds is different from the initial lamp black particles. Yet, the C-H stretching bands of aliphatic chains (2850 and 2925 cm^{-1}), the stretching bands of aromatic rings (υ C=C ~ 1540 and 1600 cm^{-1}), and aromatic C-H stretching (υ CH aromatic at 3030 cm^{-1}) are still observed, with a different intensity balance. If the residual carbon compounds are dominated by aliphatic species, they also contain aromatic hydrocarbons. The layer of organic carbon after laser cleaning is also thinner, since all the infrared bands have strongly decreased in intensity. Molecular organic compounds were also identified recently by Papanikolaou et al. [21] through their fluorescence contribution to the Raman signal of laser-cleaned marbles. These compounds are eventually bleached upon UV-B exposure, as barely no corresponding absorbance bands are detected in Area 3 (Fig. 4b). They are likely below the detection limit, as some remaining signal of the corresponding C-H groups is observed in the 1300-1600 cm^{-1} region of Area 3 (Fig. 4a). In this spectral region, a decrease of the infrared signal is also observed with the treatments, but less markedly than in the C-H stretching region.

The SEM observation of Area 1 reveals that the gypsum plate is made of a mixture of prismatic, lamellar to acicular crystals with sharp edges entangled together (Fig. 5a). The lamp black particles lie on the crystals and consist of aggregates of submicronic spherical particles (Fig. 5a and b). Some parts of the substrate remain uncovered, as already inferred from the XPS data (Fig. 2a, Area 1). On the laser cleaned surface (Area 2), the same mixture of prismatic, lamellar and acicular gypsum crystals is observed (Fig. 5c), but the lamp black aggregates have disappeared. Single submicronic round particles are sometimes detected (Fig. 5d, arrow), in rare places where the surface of the gypsum crystals is altered. This occurs probably when the crystals are not covered with lamp black particles, and consequently absorb all the laser energy.

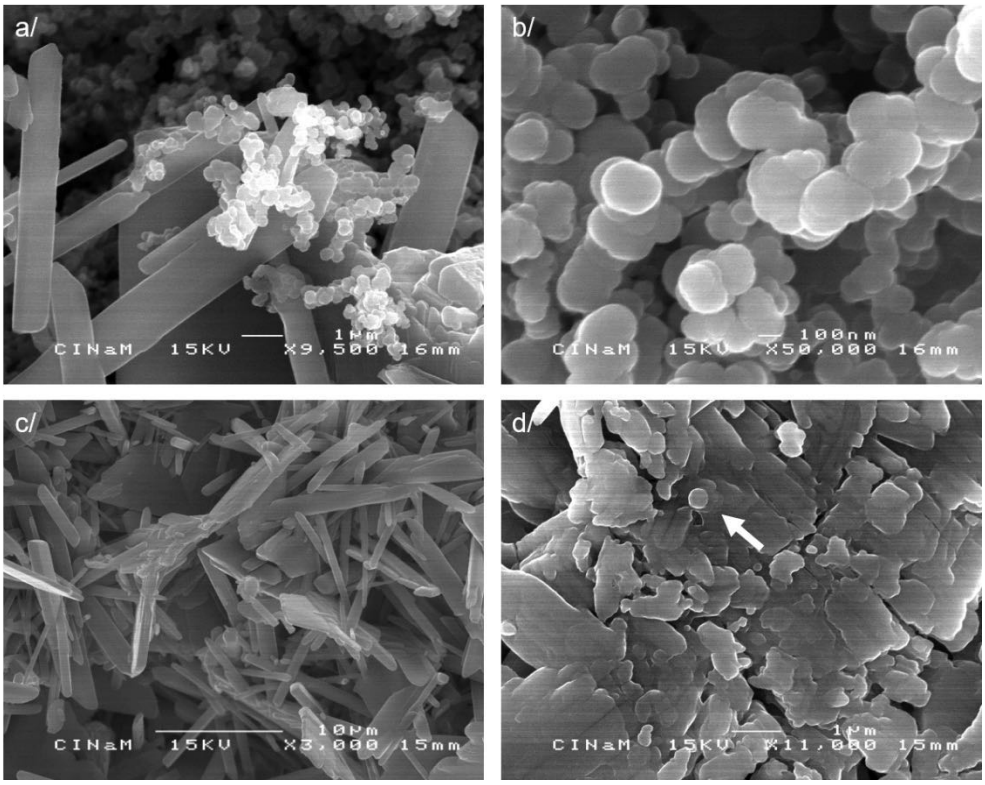

Figure 5. SEM micrographs of gypsum covered with lamp black before (Area 1) and after Q-S laser cleaning (Area 2) obtained in secondary electron mode. a/ Surface of the plaster plate showing gypsum crystals covered with aggregates of lamp black particles (Area 1). b/ Aggregates of lamp black particles of spherical shapes (Area 1). c/ Surface of the plate after Q-S laser cleaning (Area 2). d/ Details of the gypsum crystal where some alterations are observed (Area 2).

TEM micrographs show that the lamp black particles consist of primary spherical nanoparticles arranged in aggregates (Fig. 6a). The diameter of the primary nanoparticles ranges from 50 to 200 nm (Fig. 6a and b). Higher magnification (Fig. 6c) reveals their inner structure: the dark fringes correspond to small bent graphitic layers, concentrically arranged in an onion-like structure typical of soot particles [22]. After laser treatment the ejected particles have been also analyzed at high magnification. Some of them retain this initial structure (Fig. 6d), but new kinds of particles are observed. Figs. 6e-f show a class of particles with concentric multifaceted stacks of graphitic layers (white arrow on Fig. 6f) wrapping voids. A second type of particles displays evidences of a partial destruction (Fig. 6g), where graphitic stacks (Fig. 6h and i, white arrow) coexist with an amorphous carbon phase (Fig. 6g, black arrow), and where the concentric organization is lost. These images correspond well to the observed structural and chemical changes of carbon nanoparticles upon laser annealing [23,24], which simultaneously induces the crystallization of a part of the particles and the vaporization of another part,

followed by the formation of a condensed amorphous carbon phase from the carbon evaporated in the gas phase [23].

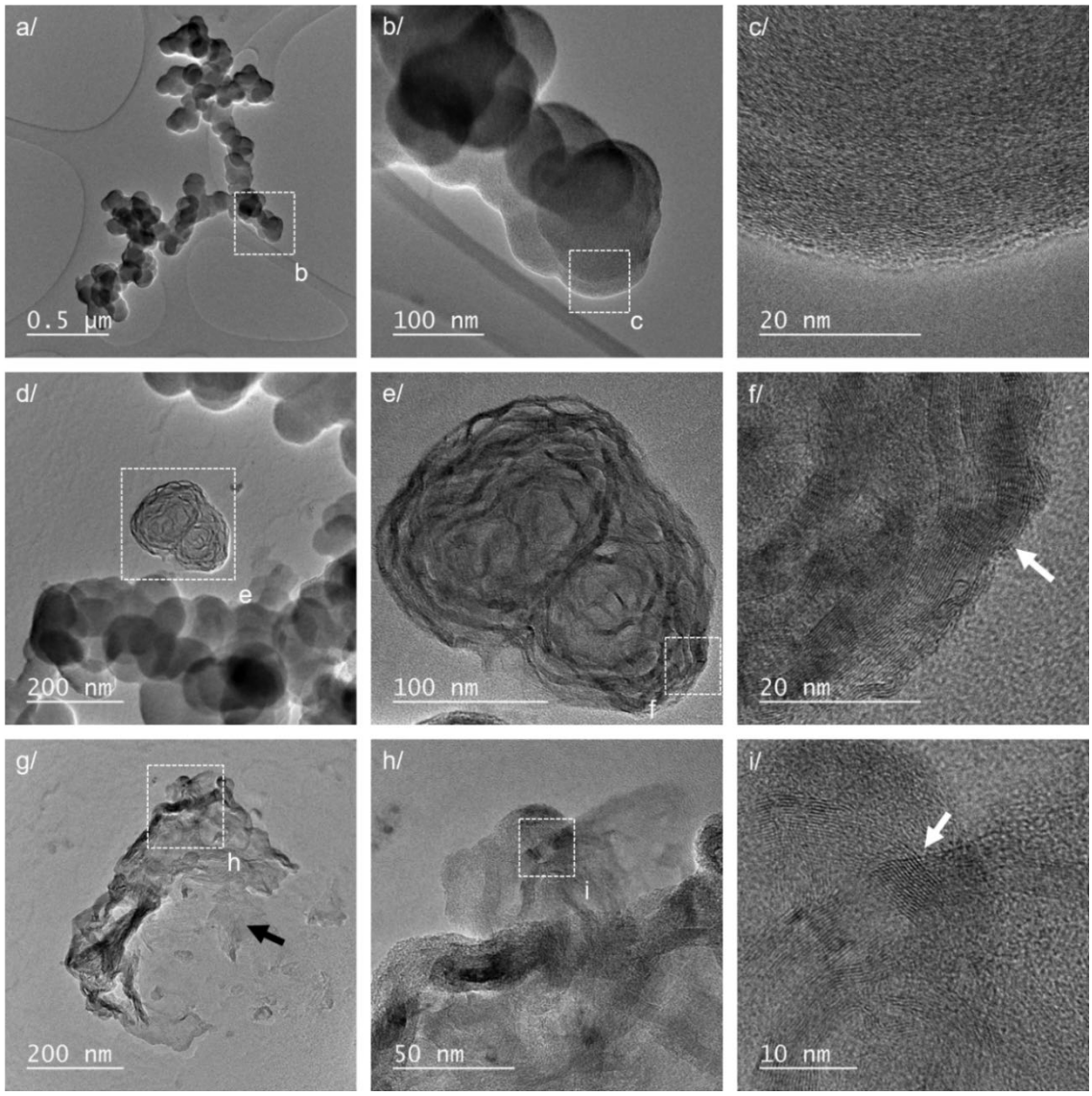

Figure 6. Structural reorganization of the lamp black particles. Bright field TEM micrographs of the lamp black particles before (a to c) and after Q-S laser cleaning (d to i). a/ to c/ aggregate composed of spherical nanoparticles, made of small graphitic planes (dark fringes) concentrically arranged. d/ to f/ aggregate of particles after laser irradiation showing alternating graphitic stacks (white arrow) and voids. g/ to i/ ablated particles with elongated and/or folded ribbon structures (white arrow) mixed with an amorphous carbon phase (black arrow).

5. Discussion

The TEM observations of the ejected particles indicate that the lamp black aggregates have been processed at very high temperatures under the laser beam. Indeed, since the thermal diffusion length is

289 $(4D\tau)^{1/2}$ where D is the thermal diffusivity of the material and □ the laser pulse duration [25], the energy
290 of short laser pulses is mainly absorbed in a small thickness [2]. As reported by Abrahamson et al. [23],
291 annealed particles like those of Fig. 6e readily form after a single pulse at 50 mJ/cm^2 of a same Nd:YAG
292 Q-switched laser at 1064 nm, corresponding to an equivalent temperature of 2850°C. This induces the
293 stacking, the growth and the de-winkling of the graphitic planes [26], accompanied by the increase of
294 the graphitic character of the considered particles [24]. At increased number of pulses, Abrahamson et
295 al. measured a maximum temperature of 4180°C (> 4 pulses or 300 mJ/cm^2) and starts detecting C_2
296 (ethene) and C_3 (propadiene) radicals in the incandescence signal of the laser plume. However, carbon
297 vaporization already starts below 4 pulses (at 3500°C), as the authors observed solidified carbon material
298 formed by nucleation of vaporized carbon [24]. In our case, laser cleaning is achieved at pulse frequency
299 (10 Hz) and fluence (200 - 400 mJ/cm^2) conditions where both graphitization and vaporization occur.
300 This leads to various forms of the ejected carbon particles observed by TEM: multifaceted annealed
301 particles (Fig. 6e), partially annealed unstructured particles mixed with an amorphous carbon phase (Fig.
302 6g), and finally intact particles (Fig 6b).

303 On the substrate side, we have seen that within the 1 nm in depth probed by XPS, the laser treatment
304 has increased the surface temperature to a minimum of 800°C, as indicated by the decomposition of
305 calcite (Fig. 2). At such temperature, dehydration of the surface of gypsum crystals certainly occurs, as
306 this process starts around 120°C. Yet, the Ca 2p line (not shown) remains unchanged after the laser
307 treatment. In particular, no CaO species are detected, and therefore anhydrous gypsum has not thermally
308 decomposed into $CaO + SO_2 + ½ O_2$ [27]. Since this reaction starts around 1200°C, it allows estimating
309 the maximum surface temperature at 1200°C. Note however that the melting point of $CaSO_4$ is not far
310 above, at 1460°C. If the surface temperature gets close to 1460°C at some places, it is not surprising to
311 observe some altered gypsum crystals and round particles (Fig. 5d) resulting from the (partial) melting
312 of gypsum. However, since the gypsum bands in the infrared spectra remain unchanged (Fig. 3) upon
313 the laser treatment, no thermal alteration of the bulk of the gypsum substrate has occurred. This is
314 consistent with the limited thermal diffusion length of the laser pulse into the substrate (28 nm).

315 The SEM observations clearly indicate that no lamp black aggregates remain after laser cleaning.
316 Therefore, the residual carbon results from the deposition of volatile carbon species at the surface of the
317 gypsum substrate. At the laser impact, the lamp black particles explode, are vaporized, chemical bonds
318 are broken, producing a plasma mixing atoms, molecules, and ions, where gas-phase chemical reactions
319 occur. A fraction of the formed products can condense on the gypsum substrate. The resulting organic
320 compounds are not visible by SEM, but they yellow the substrate. FTIR and XPS indicate that the
321 residual carbon is made of hydrocarbon dominated by aliphatic species, mixed with few aromatic
322 species. Their organic nature is essential for the facile degradation by UV-B radiation, through
323 photooxidation of linear or cyclic aliphatic [28] and aromatic hydrocarbons [29], that would not take
324 place if they were highly graphitic or made of residual black lamp particles [30]. Literature indicates
325 that laser ablation/vaporization of carbon particles produces small gas-phase carbon clusters [31] at
326 T°<3500°C, and carbenes C_2 and C_3 at T> 4180°C (and this is probably not limited to these species)
327 [24]. In any case, the formation of hydrocarbons requires both the catenation (polymerization) of carbene
328 - a facile reaction-, and a further hydrogen addition to the formed carbon chains. Hydrogen is provided
329 by the laser dissociation of water molecules coming both from dehydration of the gypsum surface and
330 from the water sprayed by the operator before the laser cleaning. Indeed, in presence of nanoparticles,
331 water radiolysis and breakdown are caused by the secondary electrons flux generated by the visible/IR
332 laser irradiations [32,33]. Water dissociation also provides O and OH radicals allowing for oxidation
333 and hydroxylation of the carbon precursors. Since the residual carbon compounds yellow the surface,
334 they include specific species not absorbing in the 560-590 nm wavelength range. A possible candidate
335 is the carbonyl group -C=O, which causes the yellowing of organic polymers [34]. Similar to the
336 hydrogenation reactions, -C=O groups can form by oxidation of the carbon precursors. Their probable
337 low concentration makes them difficult to detect with infrared spectroscopy, and, furthermore, their
338 typical bands (1670-1820 cm^{-1}) are hidden by the bending OH vibrations of the gypsum substrate. XPS
339 would be more sensitive, but the C=O groups also lie close in energy to the CO_3 group of the calcium
340 carbonate, making their detection difficult.

This study evidences, on a model system, the contribution of hydrocarbons stemming from the laser annealing of the lamp black particles. In the actual conditions of black crust soiling artworks, this process will add to the other causes of yellowing reported in the literature so far, such as the diffusion of soluble organic compounds [5,35], and the chemical transformations of iron oxides [12].

6. Summary and conclusions

Black crust frequently covers stones and plaster of artworks in urban environments. The Nd:YAG Q-Switched laser cleaning of the soiled surfaces at 1064 nm induces however a noticeable yellowing. While this phenomenon is now mitigated by the simultaneous [21] or consecutive use of UV-B [8,11], the nature of the yellowing compounds remains unknown. The present study shows, on a model system, that the initial lamp black crust is composed of aggregates of graphitic spherical nanoparticles with matrix-bonded organic species. The Nd:YAG Q-Switched laser provokes the ablation/vaporization of these particles. Some of the ejected particles seem intact, others show signs of annealing at very high temperature, such as partial graphitization or partial destruction accompanied by amorphization. A part of the laser energy is transferred to the top surface of the gypsum substrate, causing the dissociation of the calcium carbonate contaminating the substrate, within a depth of 1 nm probed by XPS. The laser ablation of the carbon nanoparticles produces a plasma plume where carbon species can polymerize and react with hydrogen and oxygen produced by the dissociation of water, emitted by both the gypsum surface and spread by the operator. This leads to the formation of hydrocarbon chains and few aromatic species which redeposit on the substrate. The yellow color could be due to the presence of some carbonyl groups (C=O) attached to the polymeric chains. The organic nature of this residual carbon allows for its facile photooxidation under the subsequent UV-B exposure.

In the light of these results, could laser cleaning be improved? The fluence and frequency of the laser pulse are set just at the ablation threshold to allow for the removal of the particles. Yet, their vaporization occurs despite this minimum deposited energy. The water sprayed before cleaning strongly enhances the process [25], but hydrogen and oxygen radicals provided by water favor the conversion of

vaporized carbon into hydrocarbon species, and their oxidation is at the origin of the yellow color. Even at 25°C and a typical 40% relative humidity, the partial pressure of atmospheric water (9.6 Torr) might provide enough water molecules ($3.1\ 10^{17}$ molecules.cm^{-3}) for these reactions to occur if no water is sprayed by the operator. From all these considerations, avoiding the formation of such a yellowish residual hydrocarbon film after laser cleaning seems rather difficult. It makes the subsequent UV-B exposure mandatory [8,11,21].

Acknowledgments

The authors would like to thank Cecile de Oliveira and Veronique Vergès-Belmin (LRMH-USR 3224, Champs-sur-Marne, France) for their help and careful advices, and Agata Dmochowska-Brasseur (Ateliers Bouvier, Les Angles, France) for the laser cleaning of the studied samples.

References

[1] S. Siano, R. Salimbeni, Advances in Laser cleaning of artwork and objects of historical interest: the optimized pulse duration approach, Acc. Chem. Res. 43 (2010) 739-750.

[2] S. Siano, J. Agresti, I. Cacciari, D. Ciofini, M. Mascalchi, I. Osticioli, A. A. Mencaglia, laser cleaning in conservation of stone, metal, and painted artifacts: state of the art and new insights on the use of the Nd:YAG lasers, Appl. Phys. A 106 (2012) 419-446.

[3] P. Bromblet, M. Labouré, G. Orial, Diversity of the cleaning procedures including laser for the restoration of carved portals in France over the last ten years, Journal of Cultural Heritage 4 (2003) 17s-26s.

[4] J. Delivré, Laser cleaning: is there specific laser esthetics?, Journal of Cultural Heritage 4 (2003) 245-248.

[5] M. Gavino, B. Hermosin, V. Vergès-Belmin, W. Nowik, C. Saiz-Jimenez, New insights on the chemical nature of stone yellowing produced after laser cleaning, Cultural Heritage Conservation

392 and Environmental Impact Assessments by Non-Destructive Testing and Micro-Analysis, eds. Van
393 Grieken and Janssens, Taylor & Francis Group, London (2005) 149-157.

394 [6] V. Vergès-Belmin, C. Dignard, Laser yellowing, myth or reality?, Journal of Cultural Heritage 4
395 (2003) 238-244.

396 [7] V. Vergès-Belmin, M. Labouré, Poultices as a way to eliminate the yellowing effect linked to
397 limestone laser cleaning, Lasers in the Conservation of Artworks: LACONA VI Proceedings,
398 Vienna, Austria 21-25 september 2005, eds. J. Nimmrichter, W. Kautek and M. Schreiner, New
399 York Springer, (2005) 115-124.

400 [8] C. De Oliveira, P. Bromblet, A. Colombini, V. Vergès-Belmin, Medium-wave ultraviolet radiation
401 to eliminate laser-induced yellowing generated by the laser removal of lamp black on gypsum,
402 Studies in Conservation 60 (2015), S34-S40.

403 [9] C. De Oliveira, V. Vergès-Belmin, D. Demaille, P. Bromblet, Lamp black and hematite contribution
404 to laser yellowing: a study on technical gypsum samples, Studies in Conservation 61 (2015), 136-
405 145.

406 [10] M.F. La Russa, C.M. Belfiore, V. Comite, D. Barca, A. Bonnazza, S.A. Ruffolo, G.M. Crisci, A.
407 Pezzino, Geochemical study of black crusts as a diagnostic tool in cultural heritage, Appl Phys A
408 113 (2013), 1151-1162.

409 [11] M. Godet, V. Vergès-Belmin, P. Bromblet, A. Colombini, M. Saheb, C. Andraud, Fly-ash
410 contribution to Nd:YAG laser yellowing and its mitigation using UV-B light, Journal of Cultural
411 Heritage 29 (2018), 36-42.

412 [12] M. Godet, V. Vergès-Belmin, N. Gauquelin, M. Saheb, J. Monnier, E. Leroy, J. Bourgon, J.
413 Verbeeck, C. Andraud, Nanoscale investigation by TEM and STEM-EELS of the laser induced
414 yellowing, Micron 115 (2018), 25-31.

415 [13] B.J. Bachman, M.J. Vasile, Ion bombardment of polylimide films, J. Vac. Sci. Technol. A 7 (1989)
416 2709-2716.

417 [14] D.R. Baer, J.F. Moulder, High resolution XPS spectrum of calcite ($CaCO_3$), Surf. Sci. Spect. 2
418 (1993) 1-2.

419 [15] H. Estrade-Szwarckopf, XPS photoemission in carbonaceous materials: a “defect” peak beside the
420 graphitic asymmetric peak, Carbon 42 (2004) 1713-1721.

421 [16] U. Gelius, P. F. Hedén, J. Hedman, B. J. Lindberg, R. Manne, R. Nordberg, C. Nordling, K.
422 Siegbahn, Molecular Spectroscopy by Means of ESCA, Phys. Scr. 2 (1970) 70-80.

423 [17] J. Bartoll, R. Stöβer, M. Nofz, Generation and conversion of electronic defects in calcium
424 carbonates by UV/Vis light, Appl. Radiat. Isot.52 (2000) 1099-1105.

425 [18] A. Putnis, B. Winkler, L. Fernandez-Diaz, In situ IR spectroscopic and thermogravimetric study of
426 the dehydration of gypsum, Mineralogical Magazine 54 (1990) 123-128.

427 [19] P.J. Larkin, Infrared and raman spectroscopy: principles and spectral interpretation, Elsevier,
428 Oxford, 2011, pp. 73-117.

429 [20] C. Russo, F. Stanzione, A. Tregrossi, A. Ciajolo, Infrared spectroscopy of some carbon-based
430 materials relevant in combustion: Qualitative and quantitative analysis of hydrogen, Carbon 74
431 (2014) 127-138.

432 [22] P. Parent, C. Laffon, I. Marhaba, D. Ferry, T.Z. Regier, I.K. Ortega, B. Chazallon, Y. Carpentier,
433 C. Focsa, Nanoscale characterization of aircraft soot: A high-resolution transmission electron
434 microscopy, Raman spectroscopy, X-ray photoelectron and near-edge X-ray absorption
435 spectroscopy study, Carbon 101 (2016) 86-100.

436 [23] J.P. Abrahamson, M. Singh, J.P. Mathews, R.L. Vander Wal, Pulsed laser annealing of carbon
437 black, Carbon 124 (2017) 380-390.

438 [24] H.P. Michelsen, A.V. Tivanski, M. K. Gilles, L.H. van Poppel, M.A. Dansson, P.R. Buseck, Particle
439 formation from pulsed laser irradiation of soot aggregates studied with a scanning mobility particle

sizer, a transmission electron microscope, and a scanning transmission x-ray microscope, Applied Optics 46 (2007) 959-977.

[25] A.C. Tam, W.P. Leung, W. Zapka, W. Ziemlich, Laser cleaning techniques for removal of surface particulates, J. appl. Phys. 71 (1992) 3515-3523.

[26] A. Oberlin, Carbonization and graphitization, Carbon 22 (1984) 521-541.

[27] Z. Yan, Z. Wang, X. Wang, H. Liu, J. R. Qiu, Kinetic model for calcium sulfate decomposition at high temperature, Trans. Nonferrous Met. Soc. China 25 (2015) 3490−3497.

[28] J.-F. Rontani, P. J. -P. Giral, Significance of photochemical degradation of petroleum hydrocarbon fractions in seawater, Intern. J. Environ. Anal. Chem. 42 (1990) 61-68.

[29] J.M. Miller, D. Olejnik, Photolysis of polycyclic aromatic hydrocarbons in water, Wat. Res. 35 (2001) 233-243.

[30] M. Li, F. Bao, Y. Zhang, W. Song, C. Chen, J. Zhao, Role of elemental carbon in the photochemical aging of soot, Proc. Nat. Acad. Sci. 115 (2018) 7717-7722.

[31] H. Michelsen, Understanding and predicting the temporal response of laser-induced incandescence from carbonaceous particles, J. Chem. Phys. 118 (2003) 7012-7045.

[32] E.V. Barmina, A.V. Simakin, G.A. Shafeev, Hydrogen emission under laser exposure of colloidal solutions of nanoparticles, Chem. Phys. Lett. 655-656 (2016) 35-38.

[33] I. Akimoto, K. Maeda, N. Ozaki, Hydrogen generation by laser irradiation of carbon powder in water, J. Phys. Chem. C 117 (2013) 18281-18285.

[34] A.E. Krauklis, A.T. Echtermeyer, Mechanism of Yellowing: Carbonyl Formation during Hygrothermal Aging in a Common Amine Epoxy, Polymers 10 (2018), 1017.

[35] P. Pouli, M. Oujja, M. Castillejo, Practical issues in laser cleaning of stone and painted artifacts: optimization procedures and side effects, Appl. Phys. A 106 (2012) 447-464.

SUPPLEMENTARY MATERIAL

Yellowing of laser-cleaned artworks: formation of residual hydrocarbon compounds after Nd:YAG laser cleaning of gypsum plates covered by lamp black.

Jeremie BERTHONNEAU[1*], Philippe PARENT[1*], Olivier GRAUBY[1], Daniel FERRY[1], Carine LAFFON[1], Alain COLOMBINI[2], Blandine COURTOIS[1] and Philippe BROMBLET[2]

[1] Aix-Marseille Université, CNRS – UMR 7325 CINaM (Centre Interdisciplinaire de Nanoscience de Marseille), Campus de Luminy, 13288 Marseille Cedex 9, France.

[2] CICRP Belle de Mai, 21 rue Guibal, 13003 Marseille, France.

*Corresponding authors, e-mail: parent@cinam.univ-mrs.fr; berthonneau@cinam.univ-mrs.fr

S1. C1s and O1s XPS

Fig. S1 presents the C1s (left panel) and O1s (right panel) data of the bare gypsum plate (bottom), the lamp black particles (top), and those of Areas 1-3 (covered with lamp black; after laser cleaning; after laser cleaning + UV), whose C1s data are shown also Fig. 2 of the article.

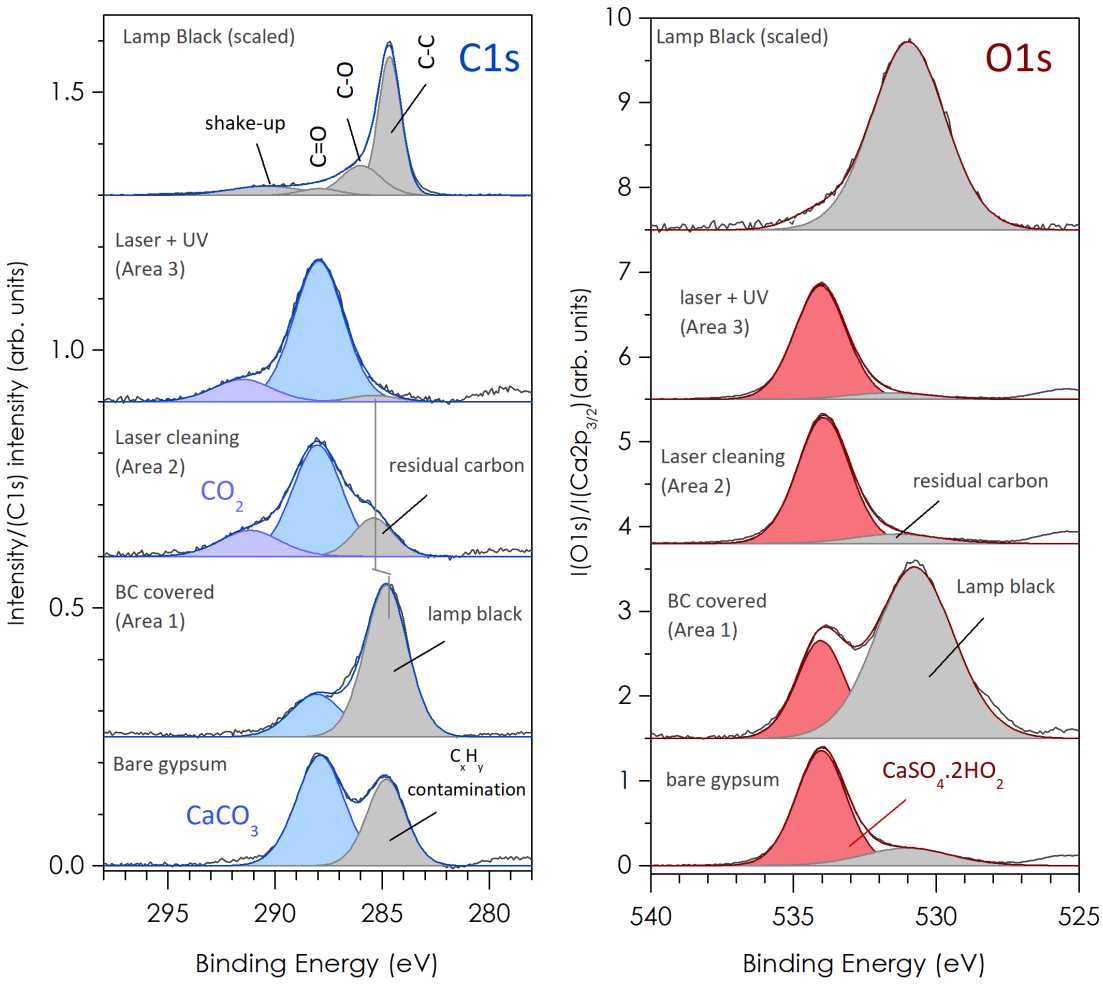

Figure S1. Deconvoluted C1s (left) and O1s (right) XPS lines of bare gypsum (bottom), of Areas 1-3 and lamp black (top).

a/ C1s XPS spectra

The C1s spectra are normalized to their integrated intensity to allow for their comparison.

-The C1s spectrum of the lamp black particles is scaled for display (left panel, top). It is deconvoluted in 4 components [1] : the most intense peak at 284.8 eV is related to C-C bonds of the graphitic layers of the primary particles. The shake-up (or plasmon) peak at 290.3 eV results from this graphitic nature. The lamp black particles are also oxidized, as shown by the two contributions of oxidized carbon at 286.0 eV (C-O) and 287.9 eV (C=O).

- The C1s spectrum of the bare gypsum plate (left panel, bottom) presents a peak at 284.8 eV, typical of adventitious hydrocarbons C_xH_y, and a second one at 288.0 eV assigned to $CaCO_3$ [2,3] contaminating the gypsum plate. This peak could hide some oxidized groups belonging to the adventitious carbon species, if any.

- The C1s spectrum of Area 1 is made of two peaks. The one at 288.0 eV is assigned to $CaCO_3$ visible through holes in the lamp black crust, and the second at 284.8 eV assigned to the lamp black peak. This peak certainly contains a (attenuated) contribution of the adventitious carbon detected on the bare gypsum plate (284.8 eV), which will also be visible through these holes. The C1s peak at 284.8 eV is fitted with a broad single component, and therefore the slight oxidized part of the lamp black spectrum is not simulated.

- The C1s spectra of Area 2 and 3 are made of three peaks. The most intense peak at 288.0 eV is the $CaCO_3$ peaks, which increases relatively to the lamp black contribution after laser cleaning (Area 2) as the particles are ablated, and after UV exposure (Area 3). As explained in the article, the second peak at 285.5 eV is assigned to the neo-formed phase of carbon that redeposits after laser ablation/vaporization (residual carbon, Area 2). The UV exposure makes it almost completely disappear (Area 3). The CO_2 peak at 291.6 eV is a side effect, due to the laser decomposition of $CaCO_3$ (see main text).

b/ <u>O1s XPS spectra</u>

The O1s spectra are normalized to the integrated intensity of the $Ca2p_{3/2}$ peak (except for lamp black) to allow for their comparison. The raw O1s spectrum of lamp black is scaled for display.

-The O1s spectrum of the lamp black particles (right panel, top) is a single peak at 530.8 eV, which includes the two contributions of the oxidized carbon groups (C=O and C-O) [4].

- The O1s spectrum of the bare gypsum plate (right panel, bottom) presents a main peak at 533.9 eV assigned to gypsum $CaSO_4.2H_2O$, that might include a weak contribution of $CaCO_3$

(energy calibration differs from [5]), and a broad one at 530.8 eV related to the oxidized carbon groups of the adventitious carbon species contaminating the gypsum plate.

- The O1s spectrum of Area 1 presents a substrate peak ($CaSO_4.2H_2O$) - pointing out from the holes of the lamp black particles-, and a contribution of the oxidized carbon groups of lamp black at 530.8 eV.

- The O1s spectra of Area 2 and 3 are made of two peaks. The most intense peak at 533.9 eV is that of gypsum $CaSO_4.2H_2O$. The peak at 530.8 eV strongly decreases after laser ablation/vaporization (Area 2). We assign it as mainly due to the oxidized part of the neo-formed phase (labelled "residual carbon"), eventually bleached after the UV treatment (Area 3).

The O1s evolution of the carbon oxide peaks from Area 1 to Area 3 is fully consistent with that of the C1s peak at 284.8 eV related to the lamp black particles contribution before/after ablation/vaporization and the subsequent UV exposure.

References

[1] H. Estrade-Szwarckopf, XPS photoemission in carbonaceous materials: A "defect" peak beside the graphitic asymmetric peak, Carbon. 42 (2004) 1713–1721. doi:10.1016/j.carbon.2004.03.005.

[2] D.R. Baer, J.F. Moulder, High Resolution XPS Spectrum of Calcite ($CaCO_3$), Surf. Sci. Spectra. 1 (2015). doi:10.1116/1.1247719.

[3] B. Demri, D. Muster, XPS study of some calcium compounds, J. Mater. Process. Technol. 55 (1996) 311–314.

[4] J.O. Müller, D.S. Su, U. Wild, R. Schlögl, Bulk and surface structural investigations of diesel engine soot and carbon black, Phys. Chem. Chem. Phys. 9 (2007) 4018–4025. doi:10.1039/b704850e.

[5] C.D. Wagner, D. Zatko, R. Raymon, Use of the Oxygen KLL Auger Lines in Identification of Surface Chemical States by Electron Spectroscopy for Chemical Analysis, Anal. Chem. 52 (1980) 1445–1451. doi:10.1021/ac50059a017.